Spin splitting of one-dimensional subbands in high quality quantum wires at zero magnetic field

K. S. Pyshkin, C. J. B. Ford, R. H. Harrell, M. Pepper, E. H. Linfield, and D. A. Ritchie
Cavendish Laboratory, Madingley Road, Cambridge CB3 0HE, United Kingdom
(Received 26 July 2000)

We have studied the transport properties of a high quality one-dimensional constriction formed in an undoped GaAs/$Al_xGa_{1-x}As$ heterostructure and therefore largely free of the random potential of ionized donors. We induce an electron gas electrostatically and are able to vary the sheet carrier density (n_{2D}) by a factor of at least seven. The constriction shows resonance-free integer conductance plateaus and the additional ''0.7 structure,'' a plateaulike feature, the conductance of which decreases from about 0.80 towards $0.5\times 2e^2/h$ at low *and* high n_{2D}. This low value is unaffected by a high in-plane magnetic field, supporting previous evidence and theories that the breaking of the spin degeneracy at high fields persists in some form, even at zero field. The height of the feature generally seen at a conductance of about $0.85\times 2e^2/h$ at high dc bias also varies, and we show that this is in reasonable agreement with a simple relation linking the conductances of the two features. We use a source-drain bias to study the spin splitting of the lowest one-dimensional subbands, and find a spin gap that is independent of n_{2D} for the first subband. We discuss possible reasons for the splitting, and show how various models for the 0.7 structure can be applied in the finite bias regime.

I. INTRODUCTION

In an ideal one-dimensional (1D) system, it has been shown that spontaneous spin polarization cannot occur in the absence of a magnetic field.[1] However, recent intriguing experimental observations of the so-called ''0.7 structure'' have suggested that this does not hold true for a quasi-1D wire.[2] When a two-dimensional electron gas (2DEG) in a semiconductor heterostructure is squeezed electrostatically with a pair of lithographically defined split gates,[3] transverse quantization into 1D subbands gives rise to conductance quantization[4] in units of $2e^2/h$. One-dimensional wires are expected to be strongly affected by electron-electron (e-e) interactions,[5,6] but these cannot usually be detected in conductance measurements.[7] However, a plateaulike feature with conductance around $0.7\times 2e^2/h$ is seen as the 1D channel depopulates, and this cannot be explained in a noninteracting picture. Similar, but much weaker features, are observed near the corresponding values for some higher index subbands. This ''0.7 structure'' has been extensively studied by Thomas *et al.* in single[2,8] and double layers,[9] and has been also observed in trench-etched GaAs quantum point contacts,[15] epitaxially gated (induced),[10,11] V-groove,[12] and quasiballistic[13] quantum wires, and in two constrictions in series.[14] The measured enhancement of the g factor as the subbands are depopulated, as well as the movement of this plateau in a strong in-plane magnetic field to $0.5\times 2e^2/h$, the value expected for a fully spin-polarized 1D level, suggest a spin-related origin of the structure.[2] By making samples with a very large 1D subband spacing, the temperature dependence was shown to be activated,[15] suggesting the presence of an excited state.

In this paper, we present measurements on a one-dimensional constriction in which the random scattering by ionized impurities is significantly reduced. The sheet density can be varied over a wide range, allowing the integer conductance plateaus and the 0.7 structure to be studied as a function of the subband spacing. We find that the conductance at which the 0.7 structure occurs decreases from about 0.80 towards $0.5\times 2e^2/h$ at low *and* high sheet densities. This low value is unaffected by a high in-plane magnetic field, implying that the breaking of the spin degeneracy at high fields persists in some form, even at zero field. The height of the ''0.85'' conductance feature generally seen at high dc bias also varies, and we show that this is in reasonable agreement with a simple, general, relation linking the conductances of the two features, provided that the mechanism causing the 0.7 structure is not significantly affected by the application of a dc bias. Spin splitting is shown to be consistent with the data, giving a spin gap that is independent of the sheet density. This may imply that, for a given sample and temperature, the 0.7 structure always occurs at about the same 1D density. A number of models for the 0.7 structure based on spin splitting are discussed, and their predictions are compared with the dc-bias data. The structure of this paper is as follows. Section II describes the techniques developed for fabricating an induced 1D electron gas. Section III presents the experimental results as a function of sheet density, in-plane magnetic field, temperature, and dc bias. In Sec. IV, we discuss a number of models which have been proposed for the 0.7 structure and consider how spin splitting should vary with dc bias. Possible mechanisms permitting spin splitting are discussed in Sec. V, together with some conclusions.

II. INDUCED ELECTRON GAS

Scattering in a 2DEG formed in a modulation-doped GaAs/$Al_xGa_{1-x}As$ heterostructure is caused mainly by potential fluctuations due to remote ionized impurities (donors), background impurities and interface roughness. In 1D, these fluctuations are much more severe,[16] and give rise to width variations and backscattering. If the doped region is removed and the 2DEG is instead induced electrostatically,[17] the scattering is greatly reduced at low densities, where screening of any donors is poor. We have developed a

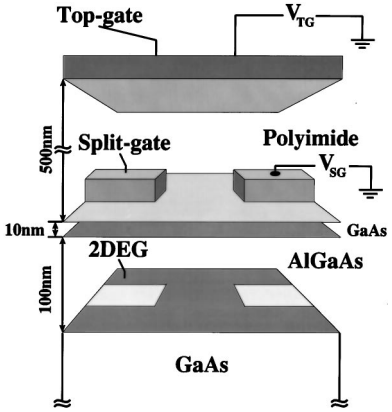

FIG. 1. Schematic diagram of the device, showing a perspective view of the various layers and the lateral gates and depletion regions.

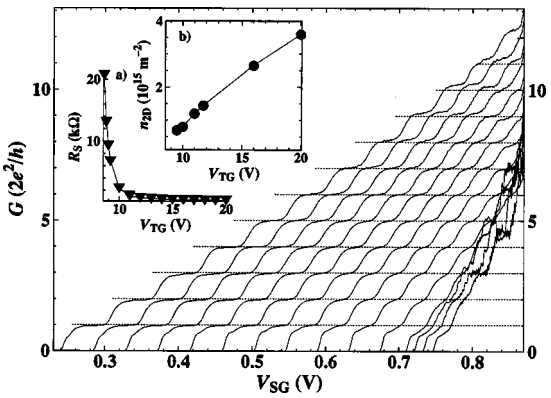

FIG. 2. The three-terminal differential conductance G of the device as a function of the split-gate voltage V_{SG} at 300 mK, after correction for series resistance R_S. The top-gate voltage V_{TG} is incremented from right to left between 8.6 V and 9.2 V in steps of 0.2 V and then between 10 V and 20 V in steps of 1 V (noise at low V_{TG} is due to the subtraction of a large R_S). Inset (a) R_S associated with one Ohmic contact drops from above 20 kΩ to below 500 Ω correspondingly. Inset (b) n_{2D} as a function of V_{TG}.

unique technique for the fabrication of such induced one- and two-dimensional electron gases.[18] In the original devices, we were able to tune the electron sheet density controllably over one order of magnitude by biasing a central surface Schottky gate (the ''mid-line''). The mobility μ was found to be much higher at low densities than in equivalent doped samples. The sample used in the present study was similar to those original devices, but the mid-line was replaced with an overall ''top'' gate above a layer of insulator, in order to minimize the channel length. The sample is shown schematically in Fig. 1.

The 2DEG is formed in a GaAs layer 110 nm below a surface Schottky gate, separated by a 100 nm undoped $Al_{0.33}Ga_{0.67}As$ barrier below a 10 nm GaAs cap. The gate is a 40 nm-thick layer of NiCr that is patterned to form a split gate with lithographic width and length 0.4 μm. The surface is then coated with a 500 nm-thick layer of polyimide, on to which a uniform ''top'' gate is deposited. Illumination with a red light-emitting diode (LED) was found to improve the quality of the 1D plateaus, probably due to a reduction in the charge trapped at the surface. The sheet carrier density (n_{2D}) varies approximately linearly with the positive bias applied to the top gate. The working n_{2D} range is between about 0.4 and 3.6×10^{15} m^{-2} as obtained from standard Hall measurements. The corresponding mobility in this wafer varies between 80 and 340 m^2/Vs, respectively, and follows the approximate relationship $\mu\propto n_{2D}^{\alpha}$, where α decreases from about 0.6 to 0.3 as n_{2D} increases. These are much lower values for α than are typically obtained in high-mobility doped heterostructures. This result shows that scattering is dominated by background impurities and interface roughness rather than by the presence of ionized impurities.[18] Thus the mobility, and the quality of the 1D channel, remain high at low densities.

III. RESULTS

A. Transport properties

Low-temperature conductance measurements were performed in a pumped He^3 cryostat using a 10-25 μV excitation voltage at a frequency of 77 Hz. All three available Ohmic contacts were used in measurements and both current and voltage were monitored using lock-in amplifiers. This ''three-terminal'' configuration excludes series resistance associated with all but one Ohmic contact and thus the necessary series resistance correction is reduced.

Figure 2 shows the conductance characteristics of the device at 300 mK. The split gate is used to open up the 1D channel, since at zero split-gate voltage (V_{SG}) the constriction is pinched off even at the highest top-gate voltage (V_{TG}) that could be applied (20 V). For $V_{SG}>0.9$ V, the split gate starts to induce an electron gas beneath it and the system becomes two-dimensional. As V_{SG} is made less positive, the 1D channel defines and gradually narrows, and the resulting depopulation of the 1D subbands causes the conductance G to decrease in a steplike manner. Twelve clean well-resolved plateaus quantized in units of $2e^2/h$ were observed. The quality of the observed conductance steps demonstrates the absence of potential fluctuations in the constriction.[19] Initial results of numerical modeling of the electrostatic potential of the constriction and $G(V_{SG},V_{TG})$ curves[20] give thresholds, capacitances, and integer plateau lengths in good agreement with the experiment.

The top-gate voltage V_{TG} was incremented to change the Fermi energy of the system. The highest 2DEG sheet density and electron mobility occur for the left-most curve on the main graph in Fig. 2, and decrease towards the right. The upper inset shows n_{2D} as a function of V_{TG}. As n_{2D} decreases, the series resistance (R_S) (from the region near one Ohmic contact) increases significantly, as shown in the lower inset, until at $V_{TG}\approx8.5$ V, the Ohmic contacts stop working. At low n_{2D} the conductance data look noisy because of the necessary subtraction of the large R_S (which is independent of V_{SG}). This disadvantage is effectively overcome in our bridging-gate devices,[18] but for the purpose of this study we prefer to have this top-gated structure, in which the 1D channel length is minimized. V_{TG} also affects the shape of the 1D electrostatic confinement. The confinement is stronger and therefore the transverse subband spacing is larger at the highest V_{TG} left-hand side (lhs), as will be shown later. Thus, the length of plateaus relative to the spacing between adjacent plateaus is larger at higher V_{TG}. For a saddle-point constric-

tion, this situation corresponds to an increased transverse curvature of the confining potential.[21] For each curve in Fig. 2 corresponding to a particular n_{2D} the one-dimensional density n_{1D} changes approximately linearly with V_{SG}. As n_{1D} decreases, *e-e* interactions may be expected to become more important, as the Coulomb energy decreases more slowly than the kinetic energy.

B. ''0.7 structure''–n_{2D} dependence

In addition to the integer conductance plateaus, we observe the additional 0.7 structure over the whole n_{2D} density range. This extends the range from that usually probed in 1D devices based on a standard doped heterostructure HEMT structure with a back gate,[2] where n_{2D} is typically changed by 30%. It is even wider than the range probed in 1D devices with a double quantum well,[9] where n_{2D} is changed by over a factor of four, covering the density range from 0.3 to 1.3 $\times 10^{15}$ m^{-2}. We change the 2DEG sheet density by at least a factor of seven (covering about three times as wide a range, but at higher density) and are therefore better able to see trends. These are summarized below.

Firstly, at the lowest achievable n_{2D}, the conductance of the 0.7 structure is close to $0.5\times 2e^2/h$ (see Fig. 2, rightmost curves). The ''knee'' (where the gradient is minimum) is at a conductance of $(0.60\pm 0.01)\times 2e^2/h$ for the lowest density trace ($n_{2D}<0.5\times 10^{15}$ m^{-2}), and the trend is still downwards as n_{2D} decreases. This is the region where *e-e* interactions are expected to be strongest and a spontaneous spin polarization has been predicted[22,23] that would result in a plateau at e^2/h. On the other hand, residual impurities are less well screened as the 2DEG sheet density is low (there are background impurities, even in induced structures). Here we have slightly overestimated the series resistance R_S (as determined by correcting the values of the higher integer plateaus) to guarantee that we are not underestimating the conductance of the feature near e^2/h. Increasing R_S further would result in an increase in the spacing of the quantized steps. Therefore, we are confident that we observe a plateau close to e^2/h in the low-n_{2D} regime. Evidence for a feature at e^2/h at low density has also been recently observed by Thomas *et al.*[9] In addition, however, we also observe that the first integer ($2e^2/h$) plateau gradually disappears with decreasing n_{2D}. This disappearance cannot easily be explained by scattering due to an impurity, since both the second and third plateaus are quite well resolved. It seems as if the increasing strength of the e^2/h feature causes the conductance to be suppressed along the whole length of what otherwise would be the $2e^2/h$ plateau.

Secondly, for intermediate n_{2D} (from about 0.7 to 2 $\times 10^{15}$ m^{-2}, corresponding to V_{TG} between 10 and 15 V, respectively) the 0.7 structure is strongest and its conductance returns to the more ''normal'' value of about 0.7 $\times 2e^2/h$ (center, Fig. 2). We have shifted the channel laterally by $\approx$50 nm here at a fixed V_{TG} by offsetting the voltage between the two arms of the split gate (not shown).[24] The quality of the plateau is unaffected by the shift, so we conclude that the structure we are following is not due to an impurity.

Finally, as the n_{2D} density is increased to about 3.6 $\times 10^{15}$ m^{-2} (our ''high-density'' regime) this structure again approaches e^2/h (left-most curves, Fig. 2). This is one of the main results of this study and the most intriguing. Indications of structure close in conductance to e^2/h at high density have recently been observed in similar, but longer, ultra-low-disorder quantum wires with a nominal length of 2 μm.[11] However, the structure was nonmonotonic rather than plateaulike, and could have been due to scattering. In our short channels, where there is no sign of disorder, it is much less likely that the structure near e^2/h can be attributed to scattering. Also, our result shows that, contrary to the suggestion by Reilly *et al.*,[11] a long wire is not crucial for the observation of structure near e^2/h.

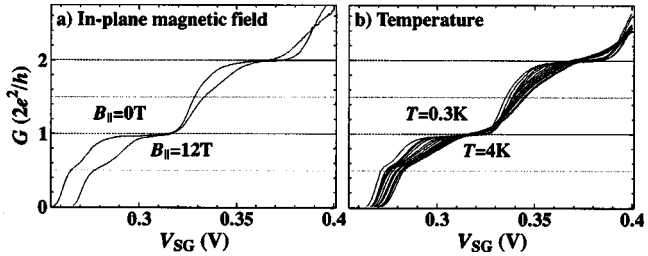

FIG. 3. (a) The conductance feature close to $0.5\times 2e^2/h$ at zero field and in a strong in-plane magnetic field $B_\parallel$ in the high-n_{2D} regime ($V_{TG}=20$ V). (b) The temperature dependence of the conductance between 0.3 and 4 K, also at $V_{TG}=20$ V. The integer plateaus become smeared out, but the feature near $0.5\times 2e^2/h$ remains strong and stays at about the same value of conductance. The pinch-off drifted slightly with time.

Very recently, another group has induced a 1DEG, using a back gate.[25] At low n_{2D}, the authors also observe a decrease in the conductance of the 0.7 structure, though at those low densities, the higher plateaus are not visible and so the increase in series resistance is unknown. At the highest n_{2D}, the behavior is unclear: the conductance of the 0.7 structure is around $0.7\times 2e^2/h$, but only one curve is shown, for $T=100$ mK. It is possible that at temperatures comparable to ours, this conductance will decrease.

C. High-density 0.5 structure–magnetic field and temperature data

To lift the spin-degeneracy of the 1D subbands, we have applied a strong in-plane magnetic field $B_\parallel$. The alignment of the sample was first adjusted by minimizing the Hall voltage arising from the out-of-plane field component, to avoid any significant change in the lateral confinement in the 1D channel. It has previously been observed that the 0.7 structure evolves into the spin-polarized plateau at e^2/h in such fields,[2,8] suggesting a possible partial spin polarization of the last subband at $B_\parallel=0$. In our case, at high density, the ''0.7'' feature becomes longer, and stays around $0.5\times 2e^2/h$ [see Fig. 3(a)], suggesting that the nearly complete spin splitting at high $B_\parallel$ persists down to $B_\parallel=0$.[9] Weak spin-splitting features do appear, as expected, midway between higher plateaus, such as at $1.5\times 2e^2/h$. At intermediate densities, the 0.7 feature has a zero-field conductance as high as 0.80 $\times 2e^2/h$, and this decreases towards $0.5\times 2e^2/h$ as $B_\parallel$ increases (it is below $0.6\times 2e^2/h$ at $B_\parallel=12$ T). At low densities, it was hard to determine the behavior as a function of magnetic field, due to the large series resistance.

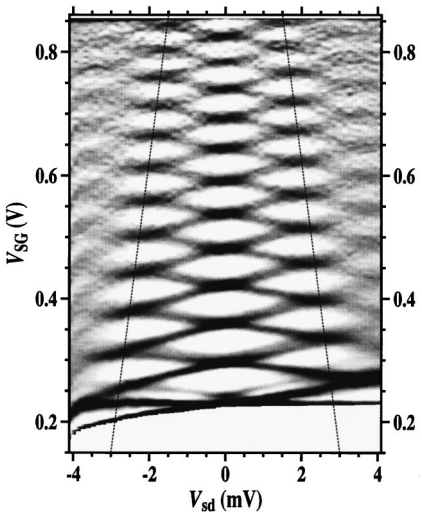

FIG. 4. Gray-scale transconductance plot as a function of the dc bias V_{sd} and of V_{SG} at $V_{TG}=20$ V. Bright regions correspond to 1D plateaus, dark lines are transconductance peaks between the plateaus. Extra lines are seen within the lower diamonds, corresponding to the riser above the 0.7 feature and its equivalents between integer plateaus. Dotted lines run through the apices of the diamond-shaped regions and represent a linear approximation to the change in the 1D subband spacing.

A change in the conductance of a plateau with temperature usually indicates thermal excitation between two levels (or between a level and the chemical potential) separated by about k_BT. Figure 3(b) demonstrates that our high-density structure near e^2/h is only slightly affected by thermal smearing and can still be seen at 4 K when the higher-index integer plateaus disappear. We cannot see a change in the conductance of the ''knee''[15] or any enhancement of the structure with increasing temperature,[2] though the conductance of the region just above the knee, including most of the first integer plateau, *is* reduced, as expected if the conductance is activated towards the ''0.7'' value.[15]

D. Energy splitting

We have probed the 1D subband energy by applying a source-drain voltage V_{sd} (dc bias).[26–28] The differential conductance G was measured by applying a small additional ac bias. According to the Glazman-Khaetskii (GK) model,[29] V_{sd} shifts the electrochemical potentials of the source (μ_s) and drain (μ_d) symmetrically in opposite directions with respect to the potential in the constriction. A peak in the transconductance dG/dV_{SG} occurs whenever the bottom of a 1D subband lines up with either μ_s or μ_d. As the source-drain voltage increases, half plateaus start to form until they completely replace the original $n\times 2e^2/h$ plateaus when the number of occupied subbands transmitted from left to right is different by one from the number going in the opposite direction.[28,36]

The transconductance is plotted in a gray-scale as a function of applied source-drain bias in Fig. 4, for $n_{2D}=3.6\times 10^{15}$ m^{-2} ($V_{TG}=20$ V), where there is a plateau close to e^2/h. Diamond-shaped bright regions represent plateaus, and dark lines correspond to transconductance peaks between them. As expected in the GK model, for the higher index

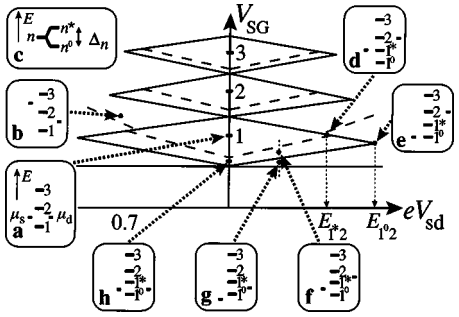

FIG. 5. Schematic diagram of the behavior of the risers between the first three 1D plateaus as a function of the dc bias V_{sd}, and of V_{SG}, as in Fig. 4. Labels 0.7, 1, 2, and 3 denote the center positions of the corresponding plateaus at $V_{sd}=0$. The insets show the relative positions in energy of the integer subbands (numbered lines) and the chemical potentials on either side of the constriction (short lines to left and right), as described in the text. Arrows show the positions in the main diagram to which the insets correspond. Level 1^0 is the first subband if there is no spin splitting, or the lower spin subband if spin splitting occurs (in models where the 0.7 structure occurs when the chemical potential lies *between* spin-split subbands); 1^* is then the upper spin subband. Inset *c* shows how the energy of the nth spin-degenerate subband may change when it is spin-split by an amount Δ_n.

subbands, half-plateaus are formed mid-way between the original $n\times 2e^2/h$ plateaus, showing that the potential is dropped symmetrically on either side of the constriction. As the 1D constriction is squeezed, the subband spacing increases, as shown by the two dotted lines in the figure. The area of the bright regions increases approximately linearly as the 1D subbands depopulate until, for the last four or three subbands, additional bright satellite regions start to form within the larger regions, and the last one becomes disproportionately larger. The whole process is illustrated schematically in Fig. 5 for the first three plateaus. The bottom line is roughly horizontal (independent of V_{SG}) because it corresponds to pinch-off ($n_{1D}=0$).

The ''anomalous'' transconductance peak (dashed line in Fig. 5), corresponding at zero dc bias to the transition from the 0.7 structure to the first integer plateau, crosses the upper edges of the lowest diamond at $eV_{sd}=E_{1^*2}$, say, and persists into the forming half-plateau region. The apex of the diamond occurs at $eV_{sd}=E_{1^02}$ (say). We show the situations with $\Delta\mu\equiv\mu_s-\mu_d=-eV_{sd}=0$ [inset (a), Fig. 5], and when $\Delta\mu$ is equal to the 1D subband spacing [inset (b)].[36] In each diagram the short bars on the left and right indicate μ_s and μ_d, respectively. Each bar in the middle represents the energy of the bottom of a 1D subband (as labeled).

In some models, the 0.7 structure occurs because the spin degeneracy of the lowest 1D subband is broken, and the chemical potential lies *between* spin-split subbands. We label as level 1^0 the first subband if there is no spin splitting, or the lower spin subband if spin splitting occurs, in which case we label the upper spin subband as 1^*. The cases where μ_d is aligned with the second 1D subband and μ_s is aligned with 1^* or with 1^0 are shown in Fig. 5 insets (d) and (e), respectively. For the nth subband, we can measure the energy difference between each of these two levels and the subband above it and thus deduce the associated energy gap $\Delta_n=E_{n^0,n+1}-E_{n^*,n+1}$ between these spin-split levels, on the

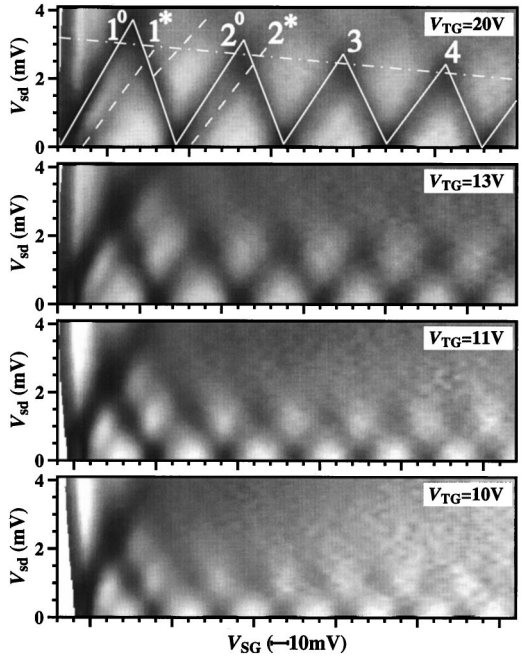

FIG. 6. Gray-scale transconductance plots as a function of V_{sd} and V_{SG} for various values of V_{TG} as labeled. For the highest n_{2D}, the figure shows lines to guide the eye, indicating the splitting of the first and second 1D subbands. The solid lines represent the risers from integer plateaus (labeled 1^0, 2^0, 3, and 4), and the dashed lines represent those from the 0.7 feature and its equivalent below the second integer plateau (labeled 1* and 2*). The dash-dotted line represents a linear approximation to the change in the 1D subband spacing.

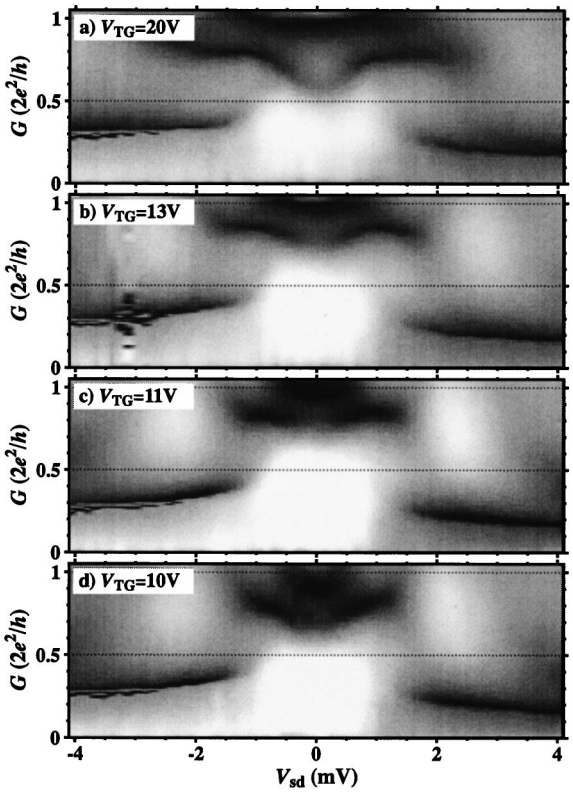

FIG. 7. Gray-scale transconductance plot as a function of V_{sd} and G for various values of V_{TG} as labeled. Dark lines correspond to plateaus. With decreasing V_{TG}, the 0.7 feature rises and then falls again at zero V_{sd}, and there is a corresponding movement in the ''0.85'' structure around $V_{sd}=\pm 1.5$ mV.

assumption that it does not depend on the position of the levels relative to μ_s or μ_d. E_{1^02} and E_{1^*2} for the first subband are shown in Fig. 5. This splitting is illustrated in inset (c) for subband n. Insets (f) and (g) show the situation at other representative points: the high dc-bias region to which inset (f) is linked generally corresponds to a plateau around $0.85\times 2e^2/h$; similarly, inset (g) is linked to a plateau around $0.35\times 2e^2/h$. In each case, one of the chemical potentials lies within the energy gap Δ_1. When both μ_s and μ_d lie within this gap (at very low dc bias), the conductance is on the 0.7 ''plateau'' [see inset (h)]. Reasons for these particular values of conductance will be discussed in Sec. IV.

Gray-scale transconductance plots for various top-gate voltages are shown in Fig. 6, allowing a comparison of the energy spacings. As in Fig. 4, dark lines represent transconductance peaks. For the highest n_{2D}, the figure shows lines to guide the eye, indicating the splitting of the first and second levels. Increasing V_{TG} increases n_{2D} and changes the shape of the potential in the constriction. The confinement increases, as shown by the measured increase in the subband spacing (proportional to the height of the diamonds in Fig. 6). This is because the required V_{SG} for a certain plateau becomes more negative. The first right-moving peak in each plot is always split, giving an extra peak that corresponds to the riser between the ''0.7'' and 1 plateaus. The splitting is more noticeable for the lowest n_{2D} (bottom graph) as the subband spacing is smallest there. For $V_{TG}=10$, 11, 13, and 20 V, we measure the spin splitting $\Delta_1=E_{1^02}-E_{1^*2}=1.08\pm 0.02$, 1.09 ± 0.02, 1.15 ± 0.07, and 1.1 ± 0.2 meV, respectively. Thus we find that the energy gap is constant, within the error, even though n_{2D} varies by nearly a factor of 5 over this range of V_{TG}, and the spacing between the first and second subbands varies from 2 to 3.5 meV. Note that equivalent energy gap Δ_2 for the second 1D level is lower, at about 0.6–0.7 meV, measured for $V_{TG}=20$ V. For higher subbands, the gap, if present, is much smaller than this. We note that Thomas *et al.*[2] found similar apparent zero-field energy gaps of 1.1 and 0.43 meV for the first and second subbands, respectively, in a doped sample at 50 mK, by calibrating the gate-voltage splitting using the dc bias. However, their gray-scale plots also yield values for Δ_1, of about 2 meV. This is not surprising, because the splitting in gate voltage between the transconductance peaks on either side of the 0.7 structure is often much larger at high V_{sd} than at $V_{sd}=0$ (where it may even be zero at low temperature).[2,30] Thus, the dc bias and thermal energy are in some way equivalent, so that the structure is visible at high bias even if the temperature is too low for it to be apparent at zero bias.[2,15,30]

The measurements are consistent with the assumption that each of the lower 1D subbands is split in energy into two spin-split levels n^* and n^0, each contributing up to e^2/h to the conductance. The possible reasons for this splitting will be discussed below.

In Fig. 7(a), the transconductance data of Fig. 4 are replotted as a function of G (and V_{sd}) rather than of V_{SG}. The anomalous transconductance peak of Fig. 4 separates the $n=1$ plateau from the 0.7 structure with close to e^2/h con-

ductance [dark bands in Fig. 7(a)]. Figures 7(b), 7(c), and 7(d) show the transconductance for lower top-gate voltages. The relative heights of the various features will be compared in the next section.

IV. MODELS

The conductance of the 0.7 structure varies significantly in Fig. 2, reflecting the change with gate voltage of a number of properties of the constriction, such as 1D density, the shape of the confining potential, impurity screening, and the energy of the bottom of the lowest 1D subband relative to the chemical potential. A parameter ξ (taking values between 0 and 1) can be introduced to describe this variation, giving the conductance of the 0.7 structure as $G_{0.7}=1/2+\xi/2$ [or equivalently, $G_{0.7}=\xi+(1-\xi)/2$]. Throughout this section we work in units of $2e^2/h$.

It is useful to consider what one might expect to see as a function of dc bias, for an arbitrary model, in order to know whether good agreement with one particular model is meaningful. At zero bias, the three lowest plateaus are $G=0$, $G=G_{0.7}$, and $G=1$. In each case, the chemical potential is related in a particular way (specific to that model) to the 1D subband structure, to yield the appropriate conductance. When a bias is applied, the energy levels in the channel stay fixed relative to the average chemical potential (assuming a symmetric potential drop), and so modulation of one sample lead is equivalent to modulation of each lead with half the amplitude, with the energy levels in the constriction kept constant. Let us therefore consider separately the contribution to the differential conductance of the modulation of the chemical potentials μ_s and μ_d on the two sides. As μ_s moves relative to the 1D subband structure, the usual plateaus occur (with half the conductance), and similarly for μ_d. Thus, a new plateau is seen when each of μ_s and μ_d gives a plateau. For example, when the contributions to the conductance from source and drain are $G_{0.7}/2$ and 1/2, respectively, the total conductance is $G_{0.85}\equiv G_{0.7}/2+1/2=3/4+\xi/4$. Similarly, when the contributions are 0 and $G_{0.7}/2$, the total conductance is $G_{0.35}\equiv 0+G_{0.7}/2=1/4+\xi/4$ (when $G_{0.7}=0.7$, $G_{0.35}=0.35$).

These two plateaus are indeed seen in all dc-bias data (see Fig. 7).[28,2,15,30] In Fig. 7(a), at high density, $G_{0.7}=0.56\pm0.02$, so $\xi=0.12$, and $G_{0.85}=0.78\pm0.01$, in good agreement with the measured height of the anomalous feature at $V_{sd}\approx\pm1.5$ meV, 0.77 ± 0.02. In Fig. 7(b), at intermediate density, $G_{0.7}=0.75\pm0.03$, so $G_{0.85}=0.875\pm0.015$, close to the measured height of 0.84 ± 0.02. Figures 7(c) and (d) show the same qualitative behavior, an increase (c) and then a decrease (d) in the conductance of the ''0.85'' feature that follows the changes in height of the zero-bias ''0.7'' feature. However, even allowing for the difficulty in determining the height of the latter, in Figs. 7(b), 7(c), and 7(d), the 0.7 feature seems slightly higher than expected from the height of the corresponding 0.85 feature. This may be due to the low temperature (300 mK) at which the measurements were performed—at higher temperature the zero-bias plateau would have occurred at a slightly lower value, more in agreement with that calculated from the value of the 0.85 structure. There is also a plateau near $G=0.35$, as expected from this analysis for $G_{0.35}$, but the height does not appear to change with $G_{0.7}$, and it also varies with V_{sd}. It is thus difficult to know which value to take when comparing with $G_{0.7}$. However, at the very smallest negative bias at which it is visible, there is a slight change in height that follows $G_{0.7}$, though the range is only one third of that expected from the movement of the 0.85 feature.

This analysis assumes that the occupation of states on, or coming from, one side does not affect the subband structure as seen by states coming from the other side, or at least that the conductance of those states remains unchanged. This cannot be the case all the time. For example, no 0.5 plateau is ever seen at high bias, whereas it should occur when the contribution to the conductance from the source is 0 and that from the drain is 1/2. Nevertheless, it would appear that our analysis should be applicable most of the time to the models that will now be described.

In one class of model, it is assumed that the lowest 1D subband is spin split, with the chemical potential lying between the two spin-split subbands when the 0.7 structure occurs. In one model, this splitting may only exist part of the time, with the system being spin degenerate (unpolarized) for a fraction ξ of the time. $G_{0.7}$ is then the time-averaged conductance of these two configurations.[31] Switching occurs between the spin-degenerate many-body ground state, with conductance $G=1$, and the thermally-activated, spin-split metastable configuration with all electrons of one spin reflected, and hence $G=\frac{1}{2}$. Instead, the roles of the states may be reversed if spin splitting is energetically favorable, with the spin-split configuration becoming the ground state. Alternatively, in an early model, based on a Tomonaga-Luttinger liquid, a spin-up mode below the chemical potential is hybridized with a spin-down mode above it.[32] This may give a plateau between 0.5 and 1. In another model, the system may be unpolarized, but nontrivial spin textures may exist in the channel for a fraction $(1-\xi)$ of the time, reflecting electrons of a particular spin.[33]

The behavior with dc bias has already been described for an excited state, at the end of the previous section and in Fig. 5. In terms of the above models, that excited state is a single-particle excitation across a spin gap to an upper spin state, and the bottoms of the unpolarized and lower-spin subbands in the two configurations are taken to have the same energy relative to the chemical potential (at least when they line up with it at zero bias). This is because n_{1D} is the same in each configuration, so the two subbands must start to fill at the same gate voltage. These models seem consistent with dc-bias and magnetic-field data, but not with thermopower measurements,[31] which show a plateau rather than a dip, coinciding with the 0.7 conductance plateau. The latter results indicate that, at the chemical potential, the transmission coefficient through the constriction is not independent of energy, and so the chemical potential cannot lie in a gap between subbands.[31]

Another model assumes spin-split subbands, both *below* the chemical potential μ. The upper one is close to μ and so is only partially occupied due to thermal depopulation.[34] This phenomenological model predicts a quasiplateau at $G=0.75$, but this value can be decreased towards 0.5 by taking a transmission coefficient less than unity, to match the conductance of the 0.7 structure better. ξ thus depends on both the Fermi function and the transmission coefficient, evalu-

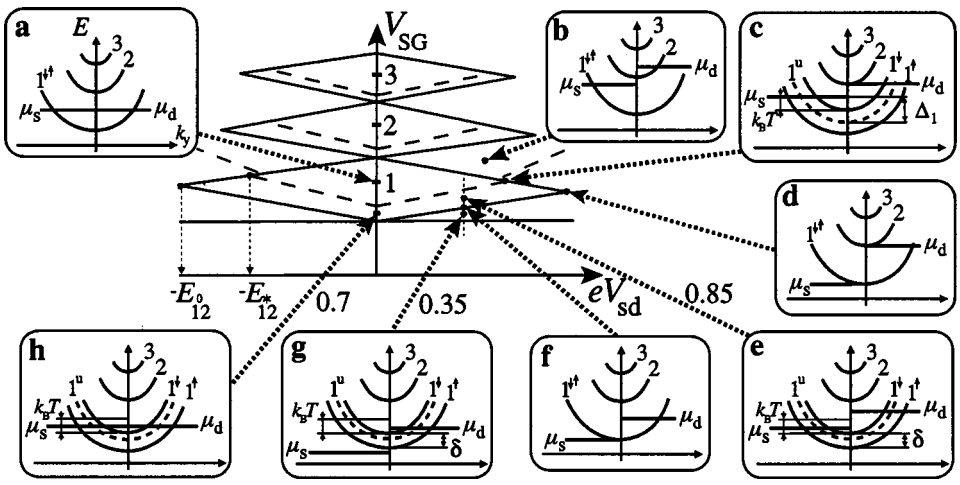

FIG. 8. Schematic diagram of the dc-bias behavior following the model of Bruus *et al.* (Ref. 34). The main diagram is as in Fig. 5. The insets show the energy E as a function of momentum k_y along the channel for each subband. The horizontal lines represent the chemical potentials μ_s and μ_s in the reservoirs at either end of the channel. Arrows show the position in the main diagram to which the inset corresponds. According to the model, the spin splitting of the lowest subband depends strongly on the relative positions of the chemical potential and the *upper* of the two spin-split subbands (labeled $1^{\uparrow}$), with no splitting if the chemical potential lies below, or many k_BT above, this subband. The lower spin-split subband is labeled $1^{\downarrow}$, and the dashed line shows the expected position 1^{u} of the first spin-degenerate subband if there were no spin splitting. Labels 0.7, 0.35, and 0.85 denote the values of the conductance features indicated by the arrows beside them. See text for details.

ated near the bottom of the upper-spin subband. The latter is pinned just below the chemical potential due to its large density of states.[35] As the chemical potential drops, the spin splitting is assumed to decrease, so that the two subbands merge just as they become completely depopulated. This is a many-body ground state, in which the system minimizes its total energy by having different occupations of the two spin-split subbands. The model appears to match much of the published experimental data quite well,[34] though the temperature dependence of the spin splitting and pinning is as yet unclear.

Using this model, it is possible to explain many aspects of the dc-bias behavior. Figure 8 shows what the model should give at various dc biases in the terms of the spin-split subbands. The main diagram is as in Fig. 5. Each inset shows the energy as a function of the wave vector k_y along the channel, for the lowest subbands. The lines labeled μ_s and μ_d indicate the chemical potentials up to which states are filled when coming from the left or right, respectively.[26] Insets (a) and (b) in Fig. 5 show situations with no spin splitting, since μ_s and μ_d are in between subbands, giving rise to the first integer plateau at $V_{sd}=0$ and a half-plateau ($G=1.5$) at finite V_{sd}, respectively. Thermal depopulation starts to occur when μ_s and μ_d come within about k_BT (multiplied by some factor) of the bottom of the first subband [inset (h), Fig. 5], giving rise to spin splitting and hence the ''0.7'' quasiplateau in conductance.[34] If just μ_s comes close to the bottom of the subband, then only the right-moving states should become thermally depopulated [inset (c), Fig. 5]. Even though the states moving to the left do not have a tendency to become spin split, we note that the other states should behave as at zero bias, developing an imbalance in the spin populations that causes spin splitting of the states moving in *either* direction, but with a smaller gap than at zero bias. (Spin splitting caused, for example, by the Coulomb interaction through an exchange effect is unlikely to depend on the direction of motion of the electrons.) As μ_s drops further, the spin splitting decreases, and the splitting of the two subbands collapses just as the right-moving states become completely depopulated [inset (d), Fig. 5].

The spin gap in (c) is *not* equal to Δ_1 as defined in Sec. III with reference to Fig. 5, which is the difference in V_{sd} of the points corresponding to insets (c) and (d) in Fig. 8, since the gap has collapsed at (d). The dashed curve in inset (c) shows approximately where in energy the spin-degenerate subband would be, if there were no splitting. The distance in energy between this curve and the subband labeled 2 is presumably very similar to that between the two lowest subbands in inset (d). Thus the measured Δ_1 is the distance shown in (c), between the dashed line and the energy above the upper-spin subband at which thermal depopulation ceases to be important (labeled k_BT above the bottom of that subband). The actual spin gap in (c) is then greater than Δ_1. By considering the 1D density of states and the thermal depopulation of the upper-spin subband, one finds that the spacing between the lower spin subband and the dashed line is greater than that between the line and the upper-spin subband, by at least a factor of about two. The actual spin gap in *c* is then greater than Δ_1, by a factor of three or more. Since the spin splitting is only driven by an imbalance in spin populations for the electrons traveling in one direction, the gap at zero bias should be even larger, perhaps also by a factor of two or more. Thus, the spin excitation gap at $V_{sd}=0$ may be at least 6 meV, for each of the top-gate voltages shown in Fig. 6. The factors should be the same in each case, so the constancy of the measured Δ_1 implies a spin gap independent of n_{2D}.

The bottom of the upper-spin subband is pinned at the chemical potential for the whole region between the dashed line and the lower border of the first diamond in Fig. 8; this region gives rise to the $G_{0.85}$ plateau in conductance described at the start of this section. The situation correspond-

ing to the middle of this plateau, with a smaller spin gap δ than that in inset (c), is illustrated in inset (e). (Note that the width in V_{sd} of the 0.85 region has been found to increase with temperature,[2] as expected in this model.) It is not clear why, in this model, this plateau should occur even when k_BT is too small for a 0.7 feature to be seen at zero bias, as described at the end of the previous section. Inset (f) shows the situation as the conductance drops below $G_{0.85}$, when the gap collapses. The spin gap should reopen when μ_d comes within k_BT of the bottom of the first subband, with μ_s below the subband. The upper-spin subband becomes pinned near μ_d, giving rise to the $G_{0.35}$ plateau [inset (g)].

This model thus seems mostly consistent with dc-bias and magnetic-field data, and with the thermopower measurements[31] mentioned above. However, it is interesting to note that, as in other models, a 0.5 plateau should occur at finite bias (for example, in inset (f) in Fig. 8 when μ_s drops below the subband), just as inset (b) gives a conductance of 1.5. This does not appear to have ever been seen experimentally. An alternative explanation for the $G_{0.35}$ plateau is that it is this 0.5 plateau, but reduced in conductance because of some asymmetry of the potential drop along the constriction[36] due to the high bias. This may explain the difference in plateau heights at positive and negative biases, and, of course, of the pinch-off voltage (Fig. 4).

V. DISCUSSION AND CONCLUSIONS

A common feature of the models of the 0.7 structure described in the previous section is the breaking of the spin degeneracy of the lowest 1D subband. This is often thought of as a complete or partial spin polarization of the electrons in the 1D channel, probably driven by the exchange interaction, forming either a new many-body ground state, or a metastable many-body state with higher total energy than the spin-unpolarized ground state, which may be occupied for only part of the time. Lieb and Mattis showed that none of this could happen for a perfect 1D wire,[1] namely one without 2D leads, and in which the second 1D subband is infinitely high in energy above the first. However, neither of these two requirements is satisfied in real samples exhibiting the 0.7 structure. The question then arises: does the relaxation of either of these formal requirements introduce a ''reason'' for the system to become polarized, rather than just making the mathematics intractable?

There may be at least one such reason. In a perfect 1D wire, all the electrons have the same transverse wave function. Thus it is impossible for electrons traveling in opposite directions to ''avoid'' each other as they pass down the wire. However, in reality, the second subband is usually only 1–10 meV above the first. For comparison, the Coulomb interaction between two particles 30 nm apart (a typical spacing along the wire), is about 4 meV. Thus, there is certainly the possibility of mixing with higher subbands. This allows the transverse wave functions to become distorted, so that electrons can, in principle, ''pass'' each other more easily. This has been seen in quantum Monte-Carlo calculations of a 1D wire.[37] It is also reminiscent of the work on systems that can be modeled as two identical, parallel 1D wires, with (antiferromagnetic) coupling between them.[38] These ''two-leg ladders'' are predicted to show a spin gap for excitations. While there is no obvious direct equivalence between the ladders and the mixed 1D eigenstates of interacting quantum wires, the work on ladders shows that making the system slightly 2D does change the physics very significantly. Theoretical calculations are hard to trust because all include exchange and correlations in some approximate way. One may have to consider many high-order corrections before the calculation converges.[1] However, various calculations have predicted spin splitting in quasi-1D wires.[22,39]

Experimentally, we have measured a spin gap (equal or proportional to Δ_1) which is independent of n_{2D}, despite the changing subband spacing. It is not clear how much n_{1D}, and hence the Coulomb energy, vary with n_{2D} in this sample. Thus, we cannot easily tell how much the intersubband mixing, and/or the spin gap, might be expected to change. The constancy of the spin gap could be taken to imply that n_{1D} is approximately the same at the point in each curve at which the 0.7 structure occurs. This is quite possible (if the degree of intersubband mixing is not important) as the second subband has not yet started to fill, and so n_{1D}, and the conductance, are determined by the distance between the bottom of the first (spin-degenerate) subband and the chemical potential, and are therefore independent of subband spacing.

At low n_{2D}, n_{1D} may be low too, increasing the Coulomb interaction energy compared with the kinetic energy. If, instead, n_{1D} is fairly constant, as described above, then intersubband mixing may be increased due to the reduced subband spacing. These mechanisms should favor the spin splitting, giving rise to the structure close to $0.5\times 2e^2/h$ that we have observed. The disappearance of the first integer plateau (Fig. 2, right-most curves) can be explained if the second subband is close to the upper spin subband of the lowest subband (with the chemical potential in between). This will occur when the subband spacing $E_{1^0 2}$ is comparable to the splitting $\Delta_1 \approx 1$ meV, shown in Figs. 5(c) and 8(c) for the two types of model that have been described. At $V_{TG} = 10$ V, $E_{1^0 2} \approx 2$ meV, and this will decrease for the curves with $V_{TG} < 10$ V, making the spacing similar to Δ_1, as required. As the upper-spin subband moves significantly below the chemical potential, so that the conductance increases from $\approx 0.5\times 2e^2/h$, tunneling through the second subband starts to occur, so that there is no first integer plateau.

At high n_{2D}, the 0.7 structure is also close to $0.5 \times 2e^2/h$. If, as mentioned above, n_{1D} at the point at which the 0.7 feature occurs is almost independent of n_{2D}, then some other parameter may be controlling the height of the feature. Relevant parameters are the subband spacing and lateral confinement, which are greatest here, and the channel length, which is likely to be slightly shorter than at lower V_{TG}.[20] This requires further experiments to investigate such a link. Alternatively, there may be a small, but nonmonotonic, variation of n_{1D}, sufficient to change the height. This is unlikely, as there is no obvious reason why the electrostatics of the system, together with the 1D density of states, should give rise to such nonmonotonicity. A third possibility is that n_{1D} increases with n_{2D}, and that, for some reason, the height of the feature actually decreases with larger n_{1D}.

The anomalous transconductance peak persists into the $1.5\times 2e^2/h$ plateau region, which forms at high dc bias (Fig. 4). This allows an interesting test for the evaluation of the energy gain or loss (if any) of the system when the propor-

tion of minority spin electrons is changing as the higher index subbands are occupied. This may shift the position of the peak once it crosses the borders of the half plateau region. There is some evidence for such a shift [see Fig. 6(a)], but further experiments are required to confirm this.

In conclusion, we have studied the transport properties of a high-quality, one-dimensional constriction, formed in an undoped $GaAs/Al_xGa_{1-x}As$ heterostructure, over a wide range of sheet densities n_{2D}. The conductance of the ''0.7 structure'' tends towards $0.5\times 2e^2/h$ at the lowest *and highest* densities, and remains there as any spin degeneracy is broken by the application of a large in-plane magnetic field. The behavior of the 0.7 structure with and without dc bias is consistent with spin splitting, and we find a spin gap that is independent of n_{2D} for the first subband. This may imply that, at least for a given sample and temperature, the 0.7 structure always occurs at about the same 1D density. We have discussed possible reasons for the splitting, and shown how various models for the 0.7 structure based on spin splitting can be applied in the finite bias regime. Much theoretical work remains to be carried out, however, to establish the physical cause of the spin splitting, and the details of its dependence on density, subband spacing, and dc bias.

ACKNOWLEDGMENTS

We thank K. J. Thomas, J. T. Nicholls, N. J. Appleyard, C. H. W. Barnes, K. A. Matveev, B. D. Simons, V. Dobrosavljevic, A. V. Moroz, and M. Kataoka for useful discussions. K.S.P. would like to acknowledge financial support from the Cambridge Overseas Trust. This work was supported by the UK EPSRC.

[1] E. Lieb and D. Mattis, Phys. Rev. **125**, 164 (1962).
[2] K. J. Thomas, J. T. Nicholls, M. Y. Simmons, M. Pepper, D. R. Mace, and D. A. Ritchie, Phys. Rev. Lett. **77**, 135 (1996); Phys. Rev. B **58**, 4846 (1998).
[3] T. J. Thornton, M. Pepper, H. Ahmed, D. Andrews, and G. J. Davies, Phys. Rev. Lett. **56**, 1198 (1986).
[4] D. A. Wharam, T. J. Thornton, R. Newbury, M. Pepper, H. Ahmed, J. E. F. Frost, D. G. Hasko, D. C. Peacock, D. A. Ritchie, and G. A. C. Jones, J. Phys. C **21**, L209 (1988); B. J. van Wees, H. van Houten, C. W. J. Beenakker, J. G. Williamson, L. P. Kouwenhoven, D. van der Marel, and C. T. Foxon, Phys. Rev. Lett. **60**, 848 (1988).
[5] S. Tomonaga, Prog. Theor. Phys. **5**, 544 (1950); J. M. Luttinger, J. Math. Phys. **4**, 1154 (1963).
[6] C. L. Kane and M. P. A. Fisher, Phys. Rev. B **46**, 15 233 (1992); M. Ogata and H. Fukuyama, Phys. Rev. Lett. **73**, 468 (1994).
[7] D. L. Maslov and M. Stone, Phys. Rev. B **52**, 5539 (1995).
[8] K. J. Thomas, J. T. Nicholls, M. Y. Simmons, M. Pepper, D. R. Mace, and D. A. Ritchie, Philos. Mag. B **77**, 1213 (1998).
[9] K. J. Thomas, J. T. Nicholls, M. Pepper, W. B. Tribe, M. Y. Simmons, and D. A. Ritchie, Phys. Rev. B **61**, R13 365 (2000).
[10] B. E. Kane, G. R. Facer, A. S. Dzurak, N. E. Lumpkin, R. G. Clark, L. N. Pfeiffer, and K. W. West, Appl. Phys. Lett. **72**, 3506 (1998).
[11] D. J. Reilly, G. R. Facer, A. S. Dzurak, B. E. Kane, R. G. Clark, P. J. Stiles, J. L. O'Brien, N. E. Lumpkin, L. N. Pfeiffer, and K. W. West, cond-mat/0001174 (unpublished).
[12] D. Kaufman, Y. Berk, B. Dwir, A. Rudra, A. Palevski, and E. Kapon, Phys. Rev. B **59**, R10 433 (1999).
[13] C.-T. Liang, M. Pepper, M. Y. Simmons, C. G. Smith, and D. A. Ritchie, Phys. Rev. B **61**, 9952 (2000).
[14] C.-T. Liang, M. Y. Simmons, C. G. Smith, G. H. Kim, D. A. Ritchie, and M. Pepper, Phys. Rev. B **60**, 10 687 (1999).
[15] A. Kristensen, P. E. Lindelof, J. B. Jensen, M. Zaffalon, J. Hollingbery, S. W. Pedersen, J. Nygard, H. Bruus, S. M. Reimann, C. B. Sorensen, M. Michel, and A. Forchel, Physica B **249-251**, 180 (1998).
[16] J. A. Nixon, J. H. Davies, and H. U. Baranger, Phys. Rev. B **43**, 12 638 (1991).
[17] B. E. Kane, L. N. Pfeiffer, K. W. West, and C. K. Harnett, Appl. Phys. Lett. **63**, 2132 (1993).
[18] R. H. Harrell, K. S. Pyshkin, M. Y. Simmons, D. A. Ritchie, C. J. B. Ford, G. A. C. Jones, and M. Pepper, Appl. Phys. Lett. **74**, 2328 (1999).
[19] K. J. Thomas, J. T. Nicholls, M. Y. Simmons, M. Pepper, D. R. Mace, and D. A. Ritchie, Appl. Phys. Lett. **67**, 109 (1995).
[20] O. A. Tkachenko, V. A. Tkachenko, D. G. Baksheyev, K. S. Pyshkin, R. H. Harrell, E. H. Linfield, D. A. Ritchie, and C. J. B. Ford (unpublished).
[21] M. Büttiker, Phys. Rev. B **74**, 33 (1996).
[22] A. Gold and L. Calmels, Philos. Mag. Lett. **74**, 33 (1996).
[23] C.-K. Wang and K.-F. Berggren, Phys. Rev. B **57**, 4552 (1998).
[24] J. G. Williamson, C. E. Timmering, C. J. P. M. Harmans, J. J. Harris, and C. T. Foxon, Phys. Rev. B **42**, 7675 (1990).
[25] S. Nuttinck, K. Hashimoto, S. Miyashita, T. Saku, Y. Yamamoto, and Y. Hirayama, Jpn. J. Appl. Phys., Part 2 **39**, L655 (2000).
[26] L. P. Kouwenhoven, B. J. van Wees, C. J. P. M. Harmans, J. G. Williamson, H. van Houten, C. W. J. Beenakker, C. T. Foxon, and J. J. Harris, Phys. Rev. B **39**, 8040 (1989).
[27] A. M. Zagoskin, Pis'ma Zh. Éksp. Teor. Fiz. **52**, 1043 (1990) [JETP Lett. **52**, 435 (1991)].
[28] N. K. Patel, J. T. Nicholls, L. Martin-Moreno, M. Pepper, J. E. F. Frost, D. A. Ritchie, and G. A. C. Jones, Phys. Rev. B **44**, 13 549 (1991).
[29] L. I. Glazman and A. V. Khaetskii, Europhys. Lett. **9**, 263 (1989).
[30] A. Kristensen, H. Bruus, A. E. Hansen, J. B. Jensen, P. E. Lindelof, C. J. Marckmann, J. Nygard, C. B. Sorensen, F. Beuscher, A. Forchel, and M. Michel, Phys. Rev. B (to be published).
[31] N. J. Appleyard, J. T. Nicholls, M. Pepper, W. R. Tribe, M. Y. Simmons, and D. A. Ritchie (unpublished).
[32] D. Schmeltzer, E. Kogan, R. Berkovits, and M. Kaveh, Philos. Mag. B **77**, 1189 (1998).
[33] V. Tripathi and D. E. Khmel'nitskii (unpublished).
[34] H. Bruus, V. V. Cheianov, and K. Flensberg, cond-mat/0002338 (unpublished).
[35] L. D. Macks, C. H. W. Barnes, J. T. Nicholls, W. R. Tribe, D. A. Ritchie, P. D. Rose, E. H. Linfield, and M. Pepper, Physica E (Amsterdam) **6**, 518 (2000).
[36] L. Martin-Moreno, J. T. Nicholls, N. K. Patel, and M. Pepper, J. Phys.: Condens. Matter **4**, 1323 (1992).
[37] F. Boltan (private communication).
[38] G. Dagotto and T. M. Rice, Science **271**, 618 (1996).
[39] C.-K. Wang and K.-F. Berggren, Phys. Rev. B **54**, R14 257 (1996).